ARCHIVES OF ACOUSTICS
26, 4, 305–329 (2001)

EVALUATION OF MATERIAL PARAMETERS, TEXTURE AND STRESS OF A PRESTRESSED POLYCRYSTALLINE AGGREGATE FROM ULTRASONIC MEASUREMENTS

J. LEWANDOWSKI

Polish Academy of Sciences
Institute of Fundamental Technological Research
(00-049 Warszawa, Świętokrzyska 21, Poland)

The propagation of ultrasonic plane waves in a polycrystalline aggregate (steel) is considered for a bulk sample of the material with plane initial (residual) stress, the material being made of cubic crystals of the highest symmetry. Some effective stiffness moduli of the bulk sample and the components of the initial stress are found as functions of the propagation velocities of the respective ultrasonic plane waves. Moreover, the use is made of Jaynes' principle of maximum Shannon entropy and the averaging procedure proposed by Voigt. In this way, the probability density function of the crystallite orientation (texture) and the effective stiffness moduli of a single crystallite of the polycrystalline aggregate are evaluated numerically for the initial plane stress increasing from zero up to about 300 MPa (in the range of elasticity). The numerical analysis shows that while the effect of the initial stress on the results of these calculations increases with increasing initial stress, the changes in the texture and effective stiffness moduli of a single crystallite are inconsiderable in the region of the values of the initial stress taken in to account.

Keywords: Polycrystalline aggregate, texture, initial (residual) stress, ultrasonic waves, elastic moduli.

1. Introduction

Polycrystalline metals are of the form of polycrystalline aggregate of numerous grains, each grain being a crystallite (monocrystal) with a single crystal symmetry of its structure and elastic properties. In general, in a macroscopic sample of the polycrystalline aggregate, which is free of initial stress and is in the so-called natural state with respect to its plastic deformation history (i.e., is in the state before its first plastic deformation), the grains are randomly oriented resulting in isotropic symmetry of the overall (effective) elastic properties of the sample. Anisotropy of the effective elastic properties and residual stress in bodies, however, usually arises from forming processes being accompanied by plastic and often nonuniform deformation. Such processes leave the crystallites in certain preferred orientations called the texture and subjects the body to a state of residual stress. The texture and residual stress induce anisotropy of the effective elastic properties, and consequently, cause variations in the speeds at which ultrasonic waves propagate through the sample, the variations depending on the directions of wave propagation and

polarization. In this context, it is natural to define the effective elastic coefficients (e.g., stiffness moduli) of a such prestressed inhomogeneous body in a well-known manner as coefficients in linearized equations of motion governing the propagation of small-amplitude elastic waves in this body, the governing equations being assumed to be of the same mathematical form as the equations governing the propagation of the waves in a bulk prestressed monocrystal with the same symmetry of the elastic properties as that of the inhomogeneous polycrystalline body under consideration. Making use of this definition, we arrive at the acoustoelastic dependencies which raise the possibility of using ultrasonics as a nondestructive technique for measurements of residual stress and evaluating some effective stiffness moduli of the bulk sample as well as for estimating the texture and the effective stiffness moduli of a single crystallite in the body. In this context, the probability density function of the crystallite orientation in such a body with non randomly oriented grains, which describes the texture, is called herein also the texture. The aim of the paper is to present the proposal of a procedure which allows us to evaluate initial (residual) stress and some effective stiffness moduli of the bulk sample as well as enable us to estimate the texture and the effective stiffness moduli of the single crystallite from the variations of the velocity of ultrasonic waves propagating through a bulk sample of a prestressed polycrystalline aggregate, which has been plasticly deformed.

The rudiments of the acoustoelastic theory, which is employed in constructing the procedure, have been developed in Refs. [1, 2]. Many practical suggestions utilized in the present paper have arisen from studying Refs. [3–5] or have their origin in these works. Proceeding in this direction, we become able to evaluate both effective stiffness moduli of the prestressed sample of the polycrystalline aggregate under consideration and the initial plane stress in that from measurements of the propagation velocities of ultrasonic waves. The second part of the problem to be solved is preparing a procedure of estimating from the same ultrasonic measurements both the texture and the effective stiffness moduli of a single crystallite in the body under consideration. The rudiments of an information theory approach are developed in this work within the framework of inversion of the VOIGT [6] concept of evaluating the effective stiffness moduli of a polycrystalline aggregate. It is well known that the essential step of utilizing the Voigt averaging procedure is calculation of the orientational volume average of functions of single crystal elastic stiffness moduli. Here the calculation of the orientational volume average denotes averaging over all crystallites in the bulk sample through the probability density function of the crystallite orientation (i.e., weighting by the probability density function). Therefore, the assumption that the Voigt concept of evaluating the effective stiffness moduli of the polycrystalline aggregate under consideration is equivalent to that based on the propagation equations and measurements of ultrasonic velocities, raises the possibility of formulating a set of integral equations with the probability density function of the crystallite orientation as an unknown function. In this context, the inversion of the Voigt procedure of evaluating the effective stiffness moduli of a prestressed polycrystalline aggregate we define as seeking the answer to the following question: for what probability density function of the crystallite orientation (texture) and for what values of the effective stiffness moduli of a single crystallite do the velocities of plane

ultrasonic waves propagating in the polycrystalline aggregate take the measured values? Formulated in such a way, the problem is ambiguous and is insoluble by using deterministic formalism. To overcome these difficulties, we make use of the probability density function of the crystallite orientation in the form implied by JAYNES [7] principle of minimum prejudice and make choice of the values of the effective stiffness moduli of a single crystallite in accordance with the minimum difference criterion, following Refs. [8, 9], respectively.

The paper is organized in the following manner. Within the framework of the formulation of the problem, basic equations, definitions, notations and concepts on acoustoelasticity are introduced in Sec. 2, the scope of the compendium being limited to that needed for formulating and solving the problem for the cases of plane initial stress different from zero and equal to zero. In Sec. 3, the theory and relevant expressions for constructing algorithms for these two cases are summarized, together with pointing out the differences between the algorithms. Controlling on line the convergence of iteration procedures and checking the exactness of numerical calculations are described in Sec. 4. Finally, numerical results obtained for steel polycrystalline aggregate with texture approximating the orthorhombic one are discussed in Sec. 5.

2. Formulation of the problem

Now a brief outline is given of the theoretical preliminaries of the proposed ultrasonic method that enable us to determine simultaneously the texture, stress and material effective parameters of a textured and prestressed polycrystalline aggregate. The solid bulk samples are assumed to be composed of a large number of cubic crystallites with the highest symmetry. In this paper, only such orientation statistics of the crystallites is considered which contributes to the orthorhombic symmetry of the effective dynamic properties of a solid bulk specimen of the polycrystalline material under examination. To discuss the orientation of a crystallite and describe all the vector and tensor quantities involved in the problem under analysis, we introduce two orthogonal reference systems. A Euler orthogonal reference system $0x_1x_2x_3$ with the axes $0x_1$, $0x_2$, and $0x_3$ is supposed to be suitably chosen, for example, in the case of a rolled plate, $0x_1$ could coincide with the rolling direction, the axes $0x_2$ and $0x_3$ being transverse to the rolling direction and normal to the rolling plane, respectively. Then the planes x_1x_2, x_2x_3 and x_3x_1 are the planes of mirror symmetry connected with the orthorhombic symmetry of the solid bulk sample. The unit vectors along the directions of the axes $0x_1$, $0x_2$, and $0x_3$ are denoted by $\mathbf{e}_1$, $\mathbf{e}_2$ and $\mathbf{e}_3$, respectively. The other orthogonal reference system $0X_1X_2X_3$ with the axes $0X_1$, $0X_2$, and $0X_3$ is supposed to be suitably chosen for a single cubic crystallite, the axes being chosen in the crystallographic directions [100], [010] and [001], respectively. The unit vectors along the directions of the axes $0X_1$, $0X_2$, and $0X_3$ are denoted by $\mathbf{E}_1$, $\mathbf{E}_2$ and $\mathbf{E}_3$, respectively. In the subsequent considerations, the orientation of a crystallite within the polycrystalline sample is described by giving the values of three Eulerian angles, θ, φ and ϕ, of the OX_1, OX_2, and OX_3 axes relative to the sample axes, Ox_1, Ox_2, and Ox_3. The notations θ ($\theta = \cos^{-1}(\mathbf{E}_3 \cdot \mathbf{e}_3)$), φ and ϕ stand for the

angle of nutation, precession and proper rotation respectively. The texture will be described by the probability density function of the crystallite orientation, $p(\xi, \varphi, \phi)$, where $\xi = \cos(\theta)$. Then $p(\xi, \varphi, \phi)\, d\xi\, d\varphi\, d\phi$ expresses the probability of a crystallite having an orientation described by the Euler angles θ $(= \cos^{-1}\xi)$, φ and ϕ, lying in the intervals $\langle \cos^{-1}\xi, \cos^{-1}(\xi + d\xi)\rangle$, $\langle \varphi, \varphi + d\varphi\rangle$ and $\langle \phi, \phi + d\phi\rangle$, respectively. The following considerations are concerned with orthorhombic bulk samples that are under applied or residual constant plane stress called the initial stress, σ^0_{ij} $(i, j = 1, 2, 3)$. It is assumed that the two principal axes of the initial plane stress, σ^0_{ij}, coincide with symmetry axes $0x_1$ and $0x_2$ of the orthorhombic material. Then the initial stress, σ^0_{ij}, does not change the symmetry and the number of independent effective elastic constants of the bulk sample under consideration. Generally, when a stress tensor σ_{ij} is referred to the reference system with the axes Ox_1, Ox_2, and Ox_3 coinciding with the principal directions of the stress σ_{ij}, then the shear stress components $\sigma_{12} = \sigma_{21}$, $\sigma_{13} = \sigma_{31}$ and $\sigma_{23} = \sigma_{32}$ vanish. Then for plane stress analysis, where the shear stress components $\sigma^0_{12} = \sigma^0_{21}$, $\sigma_{23} = \sigma_{32}$, and $\sigma_{13} = \sigma_{31}$ as well as the component σ_{33} vanish or are negligible small as compared with $\{\sigma^0_{11}, \sigma^0_{22}\}$, the only components of the initial stress, σ^0_{ij}, present in the considerations are $\{\sigma^0_{11}, \sigma^0_{22}\}$.

To be enabled to determine simultaneously the texture and initial stress σ^0_{ij} of a polycrystalline aggregate from the measurements of the propagation velocities of ultrasonic waves in a sample of the material being acted on by an ultrasonic transducer, some effective material parameters [10] must be known for characterizing both overall and single-crystal effective elastic properties. The term *effective properties* of the bulk sample under study is used to describe both the physical properties of the so-called equivalent homogeneous medium that exhibits the same symmetry of the macroscopic mechanical properties as the sample, and the so-called effective displacement response, $\mathbf{u}$, of the equivalent medium to the transducer loading. The effective displacement response is the same as the averaged displacement response of the polycrystalline material to the same loading, the averaging being carried out over a statistical ensemble of the bulk samples [8], i.e. over all crystallites through the function $p(\xi, \varphi, \phi)$. The effective dynamic properties of the prestressed orthorhombic polycrystalline aggregate under study and its single cubic crystallite (monocrystalline grain) are defined by the tensors of the effective elastic stiffness moduli, C^{eff}_{ij} and c^{eff}_{ij}, respectively. Since it is assumed that the principal axes of the initial stress, σ^0_{ij}, coincide with the symmetry axes $0x_1$ and $0x_2$ of the orthorhombic material then the initial stress, σ^0_{ij}, does not change the symmetry and the number of independent effective elastic constants of the solid bulk sample. Therefore, the non-vanishing independent effective elastic stiffness moduli of the orthorhombic polycrystalline bulk sample under consideration as well as those of a single cubic crystallite of the macroscopic sample are $\{C^{\text{eff}}_{11}, C^{\text{eff}}_{22}, C^{\text{eff}}_{33}, C^{\text{eff}}_{44}, C^{\text{eff}}_{55}, C^{\text{eff}}_{66}, C^{\text{eff}}_{12}, C^{\text{eff}}_{13}, C^{\text{eff}}_{23}\}$ and $\{c^{\text{eff}}_{11}, c^{\text{eff}}_{12}, c^{\text{eff}}_{44}\}$, respectively.

Such residual plane stresses in steel may be induced by inhomogeneous plastic deformation in some technological processes, e.g., when the steel is uniaxially rolled in cold rolling process. Then, if the axis $0x_1$ of the reference system coincides with the rolling direction, while the other axes $0x_2$ and $0x_3$ of the reference system are transverse to

the rolling direction and normal to the rolling plane, respectively, the axes Ox_1 and Ox_2 coincide simultaneously with the principal directions of the residual stress. Consequently, if the tensor σ_{ij}^0 of the residual stress is referred to the reference system with axes Ox_1, Ox_2, and Ox_3, then the shear stress components $\sigma_{12}^0 = \sigma_{21}^0$, $\sigma_{13}^0 = \sigma_{31}^0$, $\sigma_{23}^0 = \sigma_{32}^0$ vanish and if moreover σ_{33}^0 also vanishes (or at least is negligible small), the residual stress is plane. Without going into detail, the process of inducing the residual stress in the steel uniaxially rolled in cold rolling process σ_{ij}^0 may be explained after [11] as follows: The friction between the plate surface and the rolls together with plastic flow result in a complex process with the dominant component in the form of material flow process similar to sausage filling. Namely, the surfaces of the plate act as a skin, and the interior of the plate is pressed in between towards the exit side of the roll gap, the interior being in the state of compression. The compression causes also transverse material flow in the roll gap, the transverse flow being much smaller than that in the rolling direction. In this way, in the cold rolling mill, the plate becomes longer and thinner due to the plastic flow. Since all volume elements of the plate are stuck together, these length changes are absorbed partially by elastic strains, which are accompanied by the residual stresses $\{\sigma_{11}^0, \sigma_{22}^0\}$. In turn, the residual stresses are stored in the material as dislocations in the atomic lattice. If the temperature is sufficiently high, the dislocations are free to move becoming able to release the residual stresses.

In the paper, for the sake of brevity and convenience, the following tensor quantities are defined:

$$\overline{c}_{ij} = \frac{c_{ij}^{\text{eff}}}{\rho}, \qquad \overline{C}_{ij} = \frac{C_{ij}^{\text{eff}}}{\rho}, \qquad \overline{\sigma}_{11}^0 = \frac{\sigma_{11}^0}{\rho}, \qquad \overline{\sigma}_{22}^0 = \frac{\sigma_{22}^0}{\rho}. \tag{1}$$

The quantities $\overline{C}_{ij}$ and $\overline{c}_{ij}$ are used in describing the effective dynamic properties of the polycrystalline aggregate under study and its single crystallite, respectively. ρ denotes the effective density which is assumed in this paper to be equal to the density averaged over the volume of a single bulk sample. In a prestressed solid, apart from the stress σ_{ij} accompanying the strain ε_{kl} due to, e.g., the propagation of ultrasonic waves, there exists an additional initial stress σ_{ij}^0 which is accompanied by the initial strain ε_{kl}^0, both the initial quantities being assumed to be independent of time. As was mentioned, the stress σ_{ij}^0 can be both applied and residual since there is no restriction that the resulting deformations are elastic. Every $\overline{C}_{ijkl}$ is highly dependent on both microstructure and the initial stress σ_{ij}^0. For a monocrystal $C_{ijkl}^{\text{eff}} = c_{ijkl}^{\text{eff}} = c_{ijkl}$, when $\sigma_{ij}^0 = 0$.

Similar to the effective (average) density, ρ, the effective elastic moduli C_{ijkl}^{eff} are also independent of the position vector $\mathbf{x}$ (space coordinates x_1, x_2, x_3), but they are dependent on the angular frequency ω of the loading ultrasonic transducer. In contrast, the average (effective) displacement field resulting from the dynamic load with the angular frequency ω is harmonically dependent on the position vector $\mathbf{x} = (x_1, x_2, x_3)$ and time t with the same frequency ω and, consequently, is also called the effective displacement wave $\mathbf{u}$.

In the Euler coordinate system $0x_1x_2x_3$, the equations of motion for small effective elastic displacement, $\mathbf{u}$, which accompanies the propagation of an ultrasonic displacement

wave in the prestressed solid under consideration, can be written in the following form:

$$\left(\overline{C}_{ijkl} + \overline{\sigma}^0_{jl}\delta_{ik}\right) \frac{\partial^2 u_k}{\partial x_j \partial x_l} = \frac{\partial^2 u_i}{\partial t^2}, \qquad i,j,k,l = 1,2,3, \tag{2}$$

where δ_{ik} is the Kronecker tensor. Equation (2) are written by utilizing some results of Refs. [1, 2, 4, 5] under the assumption that both the material properties $\overline{C}_{ijkl}$ and the initial stress $\overline{\sigma}^0_{ij}$ vary only slightly over distances of the wavelength.

In this paper, we are interested only in the average displacement field, $\mathbf{u} = (u_1, u_2, u_3)$, in the form of a plane ultrasonic wave propagating in the direction of the unit vector $\mathbf{n} = (n_1, n_2, n_3)$ and polarized in the direction of the unit vector $\mathbf{p} = (p_1, p_2, p_3)$. Through the remainder of the paper, all equations, relations and formulae are written with locating the vector and tensor quantities relative to the $0x_1x_2x_3$ reference system. Then, $x_i = \mathbf{x}\cdot\mathbf{e}_i$, $u_i = \mathbf{u}\cdot\mathbf{e}_i$, $n_i = \mathbf{n}\cdot\mathbf{e}_i \doteq \cos(\alpha_i)$ and $p_i = \mathbf{p}\cdot\mathbf{e}_i \doteq \cos(\beta_i)$, and the wave being of interest for us may be described by the following equation:

$$\mathbf{u} = \mathbf{p}u_0 \exp\left[ik_{np}(\mathbf{n}\cdot\mathbf{x} - V_{np}t)\right] \doteq \mathbf{p}u_0 \exp\left[ik_{np}(\mathbf{n}\cdot\mathbf{x} - \omega t)\right], \tag{3}$$

where V_{np} is the phase velocity of a wave propagating in the direction of the unit vector $\mathbf{n}$ and polarized in the direction of the unit vector $\mathbf{p}$, k_{np} stands for the wave number, $k_{np} = \omega/V_{np}$ and u_0 denotes the displacement wave amplitude. The two sets of angles, $\{\alpha_i\}$ and $\{\beta_i\}$, $i = 1,2,3$, define the directions of the wave propagation and polarization, respectively.

We seek a simple particular solution to Eqs. (2) in the form given by Eq. (3). On this basis, if we put the expression given by Eq. (3) in Eqs. (2), we can infer for each pair of the propagation and polarization directions ($\mathbf{n}$ and $\mathbf{p}$) that Eqs. (2) may be solved. Moreover, the satisfaction of Eqs. (2) not only requires that, for a given polarization direction $\mathbf{p}$, the phase velocity V_{np} depends on the propagation direction $\mathbf{n}$, material parameters $\overline{C}_{ijkl}$ and initial stress $\overline{\sigma}^0_{ij}$ but also determines the form taken by the function $V_{np} = V_{np}\left(\mathbf{n}, \overline{C}_{ijkl}, \overline{\sigma}^0_{ij}\right)$. Going into detail let us remind that on substituting the plane wave solution (3) into Eqs. (2), one obtains the so-called Christoffel equations for an anisotropic material under the initial plane stress $\overline{\sigma}^0_{ij}$. If the plane stress tensor $\overline{\sigma}^0_{ij}$ is referred to the orthogonal reference system $0x_1x_2x_3$ with axes Ox_1 and Ox_2 coinciding with the principal directions of the stress $\overline{\sigma}^0_{ij}$, then, for the case under consideration, the Christoffel equations referred to the same reference system $0x_1x_2x_3$ may be expressed in the following form:

$$\left[\overline{C}_{ijkl}n_in_l + \left(\overline{\sigma}^0_{il}n_in_l - V^2_{np}\right)\delta_{jk}\right]p_k = 0 \quad \Leftrightarrow \quad A_{jk}p_k = 0, \quad i,j,k,l = 1,2,3, \tag{4}$$

where

$$\begin{aligned}
A_{11} &= \left(\overline{C}_{11} + \overline{\sigma}^0_{11}\right)(n_1)^2 + \left(\overline{C}_{66} + \overline{\sigma}^0_{22}\right)(n_2)^2 + \overline{C}_{55}(n_3)^2 - V^2_{np}, \\
A_{22} &= \left(\overline{C}_{66} + \overline{\sigma}^0_{11}\right)(n_1)^2 + \left(\overline{C}_{22} + \overline{\sigma}^0_{22}\right)(n_2)^2 + \overline{C}_{44}(n_3)^2 - V^2_{np}, \\
A_{33} &= \left(\overline{C}_{55} + \overline{\sigma}^0_{11}\right)(n_1)^2 + \left(\overline{C}_{44} + \overline{\sigma}^0_{22}\right)(n_2)^2 + \overline{C}_{33}(n_3)^2 - V^2_{np}, \\
A_{12} &= A_{21} = \left(\overline{C}_{66} + \overline{C}_{12}\right)n_1n_2, \\
A_{13} &= A_{31} = \left(\overline{C}_{55} + \overline{C}_{13}\right)n_1n_3, \\
A_{23} &= A_{32} = \left(\overline{C}_{44} + \overline{C}_{23}\right)n_2n_3.
\end{aligned} \tag{5}$$

If the system of Eqs. (4) is to have a solution different from the trivial one: every $p_k = 0$, then, in accordance with Cramer's rule, the determinant constructed from the coefficients of the A_{ij} given by Eqs. (5) must vanish. Thus we arrived at the following secular equation:

$$|A_{ij}| = 0 \tag{6}$$

which enables us to establish the above mentioned dependence of the phase velocity V_{np} on $\mathbf{n}$, $\overline{C}_{ijkl}$, and $\overline{\sigma}^0_{ij}$. Equation (6) is an equation of the third degree in V_{np} and therefore has three roots. Therefore, for any pair of unit vectors $\mathbf{n} = (n_1, n_2, n_3)$ and $\mathbf{p} = (p_1, p_2, p_3)$ we arrive at the system of Eqs. (4) – (6) and obtain three functions $V_{np} = V_{np}\left(\mathbf{n}, \overline{C}_{ijkl}, \overline{\sigma}^0_{ij}\right)$, after utilizing Cardan's solution of the cubic equation. For an ultrasonic wave given by Eq. (3) and for a vector $\mathbf{p}$, each of the three relationships defines such a form of the dependence $V_{np} = V_{np}\left(\mathbf{n}, \overline{C}_{ijkl}, \overline{\sigma}^0_{ij}\right)$, which ensure that the wave given by Eq. (3) satisfies Eqs. (2).

It is obvious that the knowledge of the three relationships, $V_{np} = V_{np}\left(\mathbf{n}, \overline{C}_{ijkl}, \overline{\sigma}^0_{ij}\right)$, enables us to construct, in the first step, an algorithm for computing some moduli $\overline{C}_{ijkl}$ and initial stress components $\overline{\sigma}^0_{ij}$ from the measurements of phase velocities V_{np}. This step is based on finding the solution with respect to $\overline{C}_{ijkl}$ of the Christoffel equation (6) and consists in applying the method proposed and developed by A.D. DEGTYAR and S.I. ROKHLIN [5] for evaluating some C^{eff}_{ijkl} and σ^0_{ij} from the nondestructive measurements of the respective ultrasonic velocities V_{np} in the polycrystalline material under examination. On finding from V_{np} the respective C^{eff}_{ijkl} of an orthorhombic polycrystalline made of cubic crystals with the highest symmetry, we are able to estimate, in the second step, the texture (i. e., to find the estimate of the function $p(\xi, \varphi, \phi)$) and all the three independent effective stiffness moduli, $\overline{c}_{11}$, $\overline{c}_{12}$ and $\overline{c}_{44}$, of a cubic crystallite. This step consists in applying the approach proposed and developed by LEWANDOWSKI [8, 9] and is based on utilization an algorithm which can be constructed by inverting the VOIGT [6] scheme of calculating $\overline{C}_{ijkl}$. Here let us remind, that the Voigt scheme consists in averaging some functions of θ, φ, ϕ, $\overline{c}_{11}$, $\overline{c}_{12}$, and $\overline{c}_{44}$ with $p(\xi, \varphi, \phi)$ as the weight function to obtain the respective effective stiffness moduli, $\overline{C}_{ijkl}$. Therefore, in the situation where $\overline{C}_{ijkl}$ can be evaluated from the measurements of V_{np} by utilizing Eqs. (4), (6), the function $p(\xi, \varphi, \phi)$ may be estimated together with $\overline{c}_{11}$, $\overline{c}_{12}$, and $\overline{c}_{44}$, by inverting the VOIGT [6] scheme of calculating $\overline{C}_{ijkl}$. However, the problem formulated in such a way is not unambiguous and the lack of uniqueness must be overcome by employing a suitable additional condition. For this reason, LEWANDOWSKI [8, 9] proposed to introduce the JAYNES' [7] principle of the maximum prejudice as a suitable additional condition and, consequently, has developed the method of estimating the function $p(\xi, \varphi, \phi)$ by inverting in the maximum-entropy approximation the Voigt averaging procedure.

Although the method proposed and developed by A.D. DEGTYAR and S.I. ROKHLIN [5] seems to be the most promising nondestructive way of evaluating $\overline{C}_{ijkl}$ and $\overline{\sigma}^0_{ij}$, great difficulty is encountered in analysis when one wishes to utilize this method for a case described by Eqs. (4) – (6) in the full form. In consequence of that, in this case all the quantities, which are to be calculated from the ultrasonic measurements, are involved in an algorithm describing relationships between them, the relationships being nonlinear and

of great complexity. Evidently, when the initial stress, $\overline{\sigma}^0_{ij}$, is not plane and its principal axes do not coincide with the symmetry and reference axes $0x_1$, $0x_2$ and $0x_3$, to which is referred the tensor of the stress σ^0_{ij}, the situation is still more complex. However, in the situation where we confine ourselves to consider a case described by Eqs. (4) – (6) with respectively chosen V_{np}, Eqs. (4) – (6) are to be used in more or less reduced form inducing in this way simplification of the algorithm. An example is presented below of such choice of a set of ultrasonic velocities V_{np} which not only enables us to evaluate $\overline{\sigma}^0_{ij}$ as well as some of moduli $\overline{C}_{ijkl}$, $\overline{c}_{11}$, $\overline{c}_{12}$ and $\overline{c}_{44}$, but also gives the possibility of estimating the function $p(\xi, \varphi, \phi)$.

Throughout the remainder of this paper, the procedure is outlined, which enable us to evaluate some $\overline{C}_{ijkl}$, $\overline{\sigma}^0_{ij}$, $\overline{c}_{11}$, $\overline{c}_{12}$ and $\overline{c}_{44}$, and to estimate the function $p(\xi, \varphi, \phi)$ in the maximum-entropy approximation. In these considerations are involved ultrasonic plane- and linearly-polarized waves that propagate in polycrystalline aggregates with orthorhombic symmetry, the aggregates being composed of crystals of the cubic class with the highest symmetry. The experimental tools for the investigations discussed in this paper are confined to the measurements of the propagation velocities V_{ij} $(i = 1, 2, 3)$ of ultrasonic plane waves propagating and polarized in the directions of the Cartesian reference axes $0x_i$ and $0x_j$, respectively, the reference axes being simultaneously the axes of the symmetry of the material bulk sample and the principal axes of the initial plane stress σ^0_{ij}. Moreover, the bulk sample is made of steel by rolling and the axis $0x_1$ coincides with the rolling direction, the other axes $0x_2$ and $0x_3$ being transverse to the rolling direction and normal to the rolling plane, respectively. Then the axes Ox_1, Ox_2, and Ox_3 coincide both with the symmetry axes of the material bulk sample (plate) and with the principal directions of the plane initial stress σ^0_{ij}. Consequently, the shear components of the initial stress, $\sigma^0_{12} = v^0_{21}$, $\sigma^0_{13} = \sigma^0_{31}$ and $\sigma^0_{23} = \sigma^0_{32}$, vanish, and two principal stress components, σ^0_{11} and σ^0_{22}, are the only nonzero initial stress components.

3. Algorithm for numerical calculations

In accordance with the earlier assumption, let us insert into Eqs. (4), (5) the ultrasonic velocities only in the form of the propagation velocities V_{ij} $(i = 1, 2, 3)$ of ultrasonic plane waves propagating and polarized in the directions of the Cartesian reference axes $0x_i$ and $0x_j$, respectively, the reference axes being simultaneously the axes of the symmetry of the orthorhombic material bulk sample and the principal axes of the initial plane stress σ^0_{ij}. This situation reduces Eqs. (4), (5) to the following simple relationships:

$$\begin{aligned} \overline{C}_{11} &= V^2_{11} - \overline{\sigma}^0_{11}\,, \qquad \overline{C}_{22} = V^2_{22} - \overline{\sigma}^0_{22}\,, \qquad \overline{C}_{33} = V^2_{33}\,, \\ \overline{C}_{44} &= V^2_{23} - \overline{\sigma}^0_{22} = V^2_{32}\,, \qquad \overline{C}_{55} = V^2_{13} - \overline{\sigma}^0_{11} = V^2_{31}\,, \qquad \overline{C}_{66} = V^2_{12} - \overline{\sigma}^0_{11}\,. \end{aligned} \tag{7}$$

Hence,

$$\overline{\sigma}^0_{22} = V^2_{23} - V^2_{32}\,, \qquad \overline{\sigma}^0_{11} = V^2_{13} - V^2_{31}\,, \qquad \overline{C}_{11} = V^2_{11} + V^2_{31} + V^2_{31} - V^2_{13}\,, \tag{8}$$

an so on.

Therefore, if the values of the eight ultrasonic velocities V_{11}, V_{22}, V_{33}, V_{12}, V_{13}, V_{23}, V_{31}, V_{32} (see Table 1) are known, the two principal stress components, σ^0_{11} and σ^0_{22}, as well as the effective material parameters $\overline{C}_{11}$, $\overline{C}_{22}$, $\overline{C}_{33}$, $\overline{C}_{44}$, $\overline{C}_{55}$, and $\overline{C}_{66}$ can be evaluated immediately from Eqs. (7), (8) but the values of the other effective material parameters ($\overline{C}_{12}, \overline{C}_{13}, \overline{C}_{23}, \overline{C}_{22}$ and $\overline{C}_{66}$) remain unattainable.

Table 1.

Input data [10^5 cm s^{-1}]								
N	V_{11}	V_{22}	V_{33}	V_{12}	V_{13}	V_{23}	V_{31}	V_{32}
1	5.93552	5.91855	5.87884	3.15212	3.22559	3.25662	3.22559	3.25662
2	5.93553	5.91855	5.87883	3.15214	3.22560	3.25661	3.22557	3.25659
3	5.93553	5.91855	5.87883	3.15217	3.22561	3.25659	3.22555	3.25656
4	5.93553	5.91857	5.87883	3.15237	3.22574	3.25644	3.22545	3.25630
5	5.93552	5.91860	5.87883	3.15262	3.22589	3.25624	3.22531	3.25596
6	5.93552	5.91862	5.87883	3.15288	3.22602	3.25605	3.22515	3.25563
7	5.93553	5.91864	5.87883	3.15312	3.22617	3.25586	3.22501	3.25530
8	5.93552	5.91877	5.87883	3.15465	3.22704	3.25472	3.22414	3.25332
9	5.93836	5.91999	5.87883	3.15796	3.23111	3.25280	3.22269	3.25000

Among the material parameters $\overline{C}_{11}$, $\overline{C}_{22}$, $\overline{C}_{33}$, $\overline{C}_{44}$, $\overline{C}_{55}$, and $\overline{C}_{66}$ involved in Eqs. (7), (8) only $\overline{C}_{33}$ can not be presented in the form of $\overline{C}_{ii} = V^2_{jk} - \overline{\sigma}^0_{mm}$ ($i = 1, 4, 5$; $j, k = 1, 2, 3$; $m = 1, 2$), but is of the form $\overline{C}_{ii} = V^2_{jk}$ only. Therefore, from all the material parameters $\overline{C}_{ii}$ involved in Eqs. (7) – (8) only $\overline{C}_{33}$ represents an entirely textural contribution to the material anisotropy, the other $\overline{C}_{ii}$ contributing to the material anisotropy due to the texture (preferred orientation of the grains) together with the initial stress σ^0_{ij}. However, in the situation where the initial stress is negligibly small or is absent, i.e., in the limiting case $\sigma^0_{ij} \to 0$, Eqs. (7) – (8) becomes a part of the system of equations describing the case when only the texture contributes considerably to the anisotropy of physical properties. This limiting case was discussed by LEWANDOWSKI in Ref. [9] where the full system of equations was outlined with utilizing some SAYERS's [3] results as well as some ultrasonic velocities were employed to predict either the texture $p(\xi, \varphi, \phi)$ in the maximum-entropy approximation and the values of some effective macroscopic parameters $\overline{C}_{ij}$ and the effective parameters $\overline{c}_{11}$, $\overline{c}_{12}$, and $\overline{c}_{44}$ of a single crystallite.

In the present paper similarly as in Ref. [9], we solve the problem of estimating the texture $p(\xi, \varphi, \phi)$ in the maximum-entropy approximation confining ourselves to inverting the averaging procedure of VOIGT [6] only. The Voigt procedure will be explained here as expressed by Eqs. (9), (10). The reason of confining ourselves in both papers to considering the case when the texture $p(\xi, \varphi, \phi)$ is estimated in the maximum-entropy approximation with using the Voigt averaging procedure only is as follows: Earlier in Ref. [8], LEWANDOWSKI compared the results of seeking the maximum-entropy estimate of the function $p(\xi, \varphi, \phi)$ for orthorhombic texture by employing in the long-wavelength approximation, the results being obtained with inverting successively the averaging procedures of VOIGT [6], REUSS [12] and HILL [13]. Moreover, the results were obtained under the assumptions that three respectively chosen velocities, V_{ij}, had been measured

and the single-crystal material parameters, c_{11}, c_{12}, c_{44} and ρ were known and did not vary (ideal polycrystalline aggregate approximation) with varying texture (due to plastic deformation). After finding the function $p(\xi, \varphi, \phi)$ from the three known ultrasonic velocities, the other six velocities, V_{ij} $(i = 1, 2, 3)$, were successively determined for each applied averaging procedure in the following two ways: from the orthorhombic symmetry conditions and by employing the maximum-entropy estimate of the function $p(\xi, \varphi, \phi)$. Next the results of calculating these velocities from both the symmetry conditions and the function $p(\xi, \varphi, \phi)$ were successively compared with each other in pairs, for each applied averaging procedure, to verify the proposed method of finding the maximum-entropy estimate of the function $p(\xi, \varphi, \phi)$ from the ultrasonic measurements. In these tests, only the velocities in each pair, in which one of the velocities was deduced from the analysis with inverting the Voigt averaging procedure, fitted the same values. This agreement in values in velocity pairs shows that the analysis with inverting the Voigt averaging procedure yields such a maximum-entropy function, $p(\xi, \varphi, \phi)$, which implies the same anisotropy of the dynamic (and propagation) properties of the polycrystalline aggregate under consideration as that deduced from the observed ultrasonic velocities by employing the othorhombic-symmetry rules. In other words, if the three respective velocities, V_{ij}, fit the measurements performed on an ideal polycrystalline aggregate with orthorhombic symmetry of the effective dynamic properties and if the maximum-entropy estimate of the function $p(\xi, \varphi, \phi)$ is deduced from this three V_{ij} by the analysis with inverting the Voigt averaging procedure, then the values of the other six velocities, V_{ij}, of ultrasonic waves propagating and polarized along the principal directions, which are calculated from the function $p(\xi, \varphi, \phi)$, also fit the respective measurements performed on the same material. As was mentioned above, in the present, paper similarly as in Ref. [9], this conclusion is the reason to confine ourselves to considering only the case when the maximum-entropy estimate of function $p(\xi, \varphi, \phi)$ is deduced by inverting the Voigt averaging procedure. In Ref. [9] was presented an approach which enables us to determine simultaneously for the limiting case $\sigma_{ij}^0 \to 0$ the effective stiffness dynamic moduli of a single grain in orthorhombically deformed steel, c_{11}^{eff}, c_{12}^{eff} and c_{44}^{eff}, some effective (overall) stiffness dynamic moduli, C_{ij}^{eff}, of the bulk sample under examination and its $p(\xi, \varphi, \phi)$, all the quantities being estimated from the measurements of ultrasonic velocities.

The algorithm of the presented numerical analysis starts with Eqs. (7), (8) which define some effective macroscopic parameters, $\overline{C}ij$, as functions of V_{ij} and $\overline{\sigma}_{i,j}^0$, c_{11}, c_{12}, c_{44}. Let us remind that, the Voigt procedure of averaging the single-crystal elastic moduli, c_{11}, c_{12}, c_{44}, enables us to evaluate the effective elastic moduli, C_{ij}^{eff}, of a bulk sample of the considered polycrystalline aggregate, the evaluation being performed under the assumption of the uniformity of strains ε_{ij} across the crystallite boundaries, i.e., under assumption that all grains are subjected to the same strain. This assumption arrives us at the following equations enabling us to calculate $\overline{C}_{ij} = c_{ij}^{\text{eff}}/\rho$:

$$\begin{aligned} \overline{C}_{ijkl} &= \langle T_{mnpq} \rangle (c_{mnpq}/\rho), \qquad T_{mnpq} = t_{im} t_{jn} t_{kp} t_{lq}\,, \\ \langle T_{mnpq} \rangle &= \int_{-1}^{1} d\xi \int_{0}^{2\pi} d\varphi \int_{0}^{2\pi} d\phi \; T_{mnpq} p(\xi, \varphi, \phi), \end{aligned} \tag{9}$$

where t_{im} denote components of the transformation matrix $\mathbf{t}(\xi, \varphi, \phi)$ which appears in the following rule of the coordinate transformation from X_j to x_i:

$$x_i = t_{ji} X_j \,. \tag{10}$$

The solutions of the Christoffel equations for an orthorhombically textured solid, which are obtained with applying the Voigt approximation (averaging procedure) to the calculation of the effective stiffness moduli of an ideal polycrystalline aggregate, are listed in Ref. [3] as formulae (10) – (21). It should perhaps be stressed that the values of the dynamic stiffness moduli c_{11}, c_{12}, c_{44} and density ρ of a single grain (crystal), were considered in [3, 8] for a deformed and textured steel as being equal to the values of c_{11}, c_{12}, c_{44} and ρ, which had been determined for a single-crystal of pure Fe with using a statical method. It is not to be expected that such an approximation, which can be called the long-wavelength and ideal Fe crystal approximation, would be always acceptable for steel, which is a polycrystalline aggregate of Fe with impurities and structure defects.

Herein is presented the next stage of the modification of seeking a complex solution to the problem of finding simultaneously c_{11}^{eff}, c_{12}^{eff} and c_{44}^{eff}, some effective stiffness dynamic moduli C_{ij}^{eff} of a prestressed orthorhombic polycrystalline aggregate, the initial stress σ_{ij}^0, and $p(\xi, \varphi, \phi)$ from the measurements of ultrasonic velocities. In the present paper, we are estimating numerically the solution to this problem in the situation where the stress σ_{ij}^0 increases from zero to a finite value. We do that in the two following ways: first, in the limiting case $\sigma_{ij}^0 \to 0$, by utilizing the approximation of small initial plane stress developed in Ref. [8, 9] and secondly, by making the use of Eqs. (7), (8) when σ_{ij}^0 is different from zero. While sketching out the main points of the enlarged numerical analysis of these problems, which is based on Eqs. (7), (8), only the concepts, definitions and equations required for following the considerations will be reiterated herein after [8, 9].

Therefore, analysing the first case when the initial stress $\sigma_{ij}^0 \to 0$, we utilize the approach proposed in Ref. [9] in seeking $p(\xi, \varphi, \phi)$ as well as c_{11}^{eff}, c_{12}^{eff}, c_{44}^{eff}, and some moduli C_{ij}^{eff}. Let us remind that in this approach [9], using [3, formulae (10) – (21)], which had been deduced from the definitions given by Eqs. (9), we arrived at the following equations [9, Eqs. (5) – (10)], after algebraic manipulation:

$$\langle r_1(\xi, \varphi, \phi) \rangle = \frac{1}{2\overline{c}} \left(\overline{c}_{11} - V_{11}^2 \right), \qquad \overline{c} = \overline{c}_{11} - \overline{c}_{12} - 2\overline{c}_{44} \,, \tag{11}$$

$$\langle r_2(\xi, \varphi, \phi) \rangle = \frac{1}{2\overline{c}} \left(\overline{c}_{11} - V_{22}^2 \right), \tag{12}$$

$$\langle r_3(\xi, \varphi, \phi) \rangle = \frac{1}{2\overline{c}} \left(\overline{c}_{11} - V_{33}^2 \right), \tag{13}$$

$$\langle r_4(\xi, \varphi, \phi) \rangle = \frac{1}{\overline{c}} \left(V_{23}^2 - \overline{c}_{44} \right), \tag{14}$$

$$\langle r_5(\xi, \varphi, \phi) \rangle = \frac{1}{\overline{c}} \left(V_{31}^2 - \overline{c}_{44} \right), \tag{15}$$

$$\langle r_6(\xi, \varphi, \phi) \rangle = \frac{1}{\overline{c}} \left(V_{12}^2 - \overline{c}_{44} \right), \tag{16}$$

where

$$r_4 = r_3 + r_2 - r_1 \,, \qquad r_5 = 2(r_1 - r_2) + r_4 \,, \qquad r_6 = 2r_1 - r_5 \,, \tag{17}$$

$$\begin{aligned} r_1 &= l_1^2 l_2^2 + l_1^2 l_3^2 + l_2^2 l_3^2\,, \qquad r_2 = m_1^2 m_2^2 + m_1^2 m_3^2 + m_2^2 m_3^2\,, \\ r_3 &= n_1^2 n_2^2 + n_1^2 n_3^2 + n_2^2 n_3^2\,, \\ l_i &= \mathbf{E}_i \cdot \mathbf{e}_1\,, \qquad m_i = \mathbf{E}_i \cdot \mathbf{e}_2\,, \qquad n_i = \mathbf{E}_i \cdot \mathbf{e}_3\,. \end{aligned} \tag{18}$$

The abbreviations $\langle r_q \rangle$, $q = 1, 2, ..., 6$, in Eqs. (11) – (16) denote averaging the functions $r_q(\theta, \varphi, \phi)$ of a single-crystal orientation defined earlier, the averaging being performed over all the crystallites in the sample, i.e. $\langle r_q(\theta, \varphi, \phi) \rangle$ is $r_q(\theta, \varphi, \phi)$ weighted by $p(\theta, \varphi, \phi)$:

$$\langle r_q(\xi, \varphi, \phi) \rangle = \int_0^{2\pi} \int_0^{2\pi} \int_{-1}^{1} r_q(\xi, \varphi, \phi) p(\xi, \varphi, \phi) d\xi \, d\varphi \, d\phi. \tag{19}$$

The probability density function $p(\xi, \varphi, \phi)$ fulfils the normalization condition

$$\langle p(\xi, \varphi, \phi) \rangle \doteq \int_0^{2\pi} \int_0^{2\pi} \int_{-1}^{1} p(\xi, \varphi, \phi) d\xi \, d\varphi \, d\phi = 1. \tag{20}$$

It should perhaps be emphasized that each left-hand side of the six equations (5) – (10) is of the form of an expectation value of one of the six known functions, $r_q(\xi, \varphi, \phi)$, of a single-crystal orientation. From these six functions, only three functions $r_q(\xi, \varphi, \phi)$ are linearly independent of each other. Each right-hand side of the six equations (5) – (10) is of the form of a known function of an ultrasonic velocity, V_{ij}, and single-crystal effective material parameters $\bar{c}_{11}$, $\bar{c}_{12}$, $\bar{c}_{44}$ defined by Eqs. (1). It can be easily seen from Eqs. (11) – (16) that each of such three velocities V_{ij}, which satisfies the rule that each of the numbers 1, 2 and 3 appear as subscripts i and/or j at no more than two velocities (e.g., V_{11}, V_{33}, and V_{31}) is involved in a formula determining the value of only one expectation value, $\langle r_q(\xi, \varphi, \phi) \rangle$, the three expectation values being linearly independent of each other. For this reason, the measurements of V_{11}, V_{33}, and V_{31} were in Ref. [8] sufficient for the probability density function $p(\xi, \varphi, \phi)$ to be *fully* estimated for aggregates with orthorhombic symmetry with known $\bar{c}_{11}$, $\bar{c}_{12}$, $\bar{c}_{44}$, and $\sigma_{ij}^0 = 0$. Essentially, then the probability density function $p(\xi, \varphi, \phi)$ implied by the JAYNES' [7] principle of maximum Shannon entropy is given in terms used in Eqs. (11) – (16) by the following expression:

$$p(\xi, \varphi, \phi) = \frac{1}{Z} \exp\left[-L_1 r_1(\xi, \varphi, \phi) - L_3 r_3(\xi, \varphi, \phi) - L_5 r_5(\xi, \varphi, \phi)\right], \tag{21}$$

where the partition function Z and the Lagrangian multipliers L_1, L_3 and L_5 are to be determined from Eqs. (11), (13), (15) and the normalization condition (20).

In Ref. [9], which concerns non-prestressed ($\sigma_{ij}^0 = 0$) aggregates with orthorhombic symmetry, the system of equations (11) – (18) was used for estimating in the maximum entropy approximation the probability density function $p(\xi, \varphi, \phi)$, unknown material parameters $\bar{c}_{11}$, $\bar{c}_{12}$, $\bar{c}_{44}$, and some $\overline{C}_{ij}$. The problem was solved in two steps for the case when the same three ultrasonic velocities V_{11}, V_{33}, V_{31} and additionally one of the velocities V_{22}, V_{23} and V_{12} are known. In the first step, the analytical form of the probability density function $p(\xi, \varphi, \phi)$ was deduced from the observables V_{11}, V_{33} and V_{31} by utilizing the JAYNES' [7] principle of maximum Shannon entropy. Consequently, the analytical

form of $p(\xi,\varphi,\phi)$ in [9] also is given by Eq. (21) but with the partition function Z and the Lagrangian multipliers L_1, L_3 and L_5, which are to be found in the second step together with the material parameters $\overline{c}_{11}$, $\overline{c}_{12}$ and $\overline{c}_{44}$, from the seven equations (11) – (16), (20) with employing the orthorhombic symmetry rules and the values of the ultrasonic velocities V_{11}, V_{33}, V_{31}, and an additional one, say, V_{23}. Since the system of equations (11) – (16), (20) for the quantities Z, L_1, L_3, L_5, $\overline{c}_{11}$, $\overline{c}_{12}$ and $\overline{c}_{44}$, which results from formulating the variational problem for the conditional maximum of missing information and inverting the Voigt averaging procedure, describes very complicated dependencies of these quantities on each other, a direct solution of the task is not available and a tedious numerical method is required to be used. A more detailed description of the operations of the program evaluating Z, L_1, L_3, L_5, $\overline{c}_{11}$, $\overline{c}_{12}$ and $\overline{c}_{44}$ was presented in Ref. [9]. To avoid making the paper even longer, any detailed description of the numerical method will not be reiterated herein after [9], although it should be stressed that the approach proposed in Ref. [9] is considered here as a suitable one only in the case when the initial stress, σ^0_{ij}, is small, i.e., in accordance with Eqs. (8), when

$$\mathrm{DABS}\left(\left(V^2_{ij}-V^2_{ji}\right)/\mathrm{DMIN}\,1\left(V^2_{ij},V^2_{ji}\right)\right)\ll 1, \qquad i,j=1,2,3, \quad i\neq j. \tag{22}$$

The nomenclature introduced in Eq. (22) is as follows: DABS denotes the FORTRAN 77 intrisinc function that returns the absolute value of its argument, DMIN1 is another FORTRAN 77 intrisinc function which returns the minimum value in the argument list. The smaller are the components of the initial stress, σ^0_{ij}, the better is the approximation of the texture of a prestressed polycrystalline obtained by using the approach proposed in Ref. [9].

In this paper, the proposed method of estimating the textural contribution to the orthorhombic acoustic anisotropy of prestressed polycrystalline aggregates ($\sigma^0_{ij}\neq 0$) is based on Eqs. (7), (8). On inserting Eqs. (9), (10) into Eqs. (7), (8), we arrive at the following system of equations, after employing [3, formulae (10) – (21)] and algebraic manipulation:

$$\langle r_1(\xi,\varphi,\phi)\rangle = \frac{1}{2\overline{c}}\left(\overline{c}_{11}-H_{11}\right), \qquad H_{11}=V^2_{11}+V^2_{31}-V^2_{13}, \tag{23}$$

$$\langle r_2(\xi,\varphi,\phi)\rangle = \frac{1}{2\overline{c}}\left(\overline{c}_{11}-H_{22}\right), \qquad H_{22}=V^2_{22}+V^2_{32}-V^2_{23}, \tag{24}$$

$$\langle r_3(\xi,\varphi,\phi)\rangle = \frac{1}{2\overline{c}}\left(\overline{c}_{11}-V^2_{33}\right), \tag{25}$$

$$\langle r_4(\xi,\varphi,\phi)\rangle = \frac{1}{\overline{c}}\left(V^2_{32}-\overline{c}_{44}\right), \tag{26}$$

$$\langle r_5(\xi,\varphi,\phi)\rangle = \frac{1}{\overline{c}}\left(V^2_{31}-\overline{c}_{44}\right), \tag{27}$$

$$\langle r_6(\xi,\varphi,\phi)\rangle = \frac{1}{\overline{c}}\left(H^2_{12}-\overline{c}_{44}\right), \qquad H_{12}=V^2_{12}+V^2_{31}-V^2_{13}. \tag{28}$$

Equations (23) – (28), (20) are the reliable basis for the maximum-entropy estimate of the orthorhombic texture of the prestressed polycrystalline aggregate from the measurements of the propagation velocities V_{ij} $(i,j=1,2,3)$ of the ultrasonic plane and linearly

polarized waves. This method consists in finding in two stages the maximum-entropy estimation of the probability density function $p(\xi, \varphi, \phi)$. Similarly to Eqs. (11) – (16), each left-hand side of Eqs. (23) – (28) is of the form of the expectation value of one of the functions $r_i(\xi, \varphi, \phi)$, $i = 1$ to 6, weighted with $p(\xi, \varphi, \phi)$, and each right-hand side of these equations is of the form of a known function of some quantities belonging to the set of the following five quantities: an ultrasonic velocity, V_{ij}, three material parameters $\bar{c}_{11}$, $\bar{c}_{12}$, $\bar{c}_{44}$ and the two (σ^0_{11} and σ^0_{22}) non vanishing components of the initial plane stress, σ^0_{ij}. From the system of Eqs. (23) – (28), (20), it can immediately be seen which of the nine ultrasonic velocities V_{ij} $(i, j = 1, 2, 3)$ should be known from the measurements for each situation under consideration. On performing the respective measurements, the two (σ^0_{11} and σ^0_{22}) non-vanishing components of the initial plane stress can be evaluated directly from Eqs. (8). The analytical form of the function $p(\xi, \varphi, \phi)$ can be determined from a system of three equations obtained by reducing the system of six equations (23) – (28) to that with three functions $r_i(\xi, \varphi, \phi)$, which are linearly independent of each other. Then the analytical form of $p(\xi, \varphi, \phi)$ can be determined from such a system of three equations by inverting in the maximum-entropy approximation the Voigt averaging procedure, which was assumed to be suitable for calculating the expectation values involved in Eqs. (23) – (28). For example, if $r_1(\xi, \varphi, \phi)$, $r_3(\xi, \varphi, \phi)$, and $r_5(\xi, \varphi, \phi)$ are chosen as the three independent of each other functions $r_i(\xi, \varphi, \phi)$, then the analytical form of the function $p(\xi, \varphi, \phi)$ is again given by Eq. (21). While the probability density function $p(\xi, \varphi, \phi)$ implied by the observables V_{11}, V_{33} and V_{31} and by the JAYNES' [7] principle of maximum Shannon entropy is also of the form given by Eq. (21) as in Ref. [9], now the partition function Z and the Lagrangian multipliers L_1, L_3 and L_5 are to be determined together with the unknown material parameters $\bar{c}_{11}$, $\bar{c}_{12}$ and $\bar{c}_{44}$ from Eqs. (23) – (28), (20), some of them being more complicated than their analogues in Ref. [9]. The increase in the complexity is due to the dependence of each of the seven unknown quantities Z, L_1, L_3, L_5, $\bar{c}_{11}$, $\bar{c}_{12}$ and $\bar{c}_{44}$ on both the texture $p(\xi, \varphi, \phi)$ and the initial plane stress $\sigma^0_{ij} = \{\sigma^0_{11}, \sigma^0_{22}\} \neq 0$.

4. Results of numerical analysis

In the subsequent numerical analysis, we seek the function $p(\xi, \varphi, \phi)$, material parameters $\bar{c}_{11}$, $\bar{c}_{12}$, $\bar{c}_{44}$, and some $\overline{C}_{ij}$ for a rolled steel plate. It is assumed that the values of the ultrasonic velocities presented in Table 1 were obtained from experiments. Moreover, it is assumed that the set of the values in each row was obtained in the same of the nine groups of measurements, each measurement of any group being performed on the same sample in the same state of the initial plane stress σ^0_{ij}. In accordance with Eqs. (7), (8), the values given in any row of Table 1 enable us to evaluate immediately the initial plane stress $\sigma^0_{ij} = \{\sigma^0_{11}, \sigma^0_{22}\} \neq 0$ and some material parameters, $\overline{C}_{11}$, $\overline{C}_{22}$, $\overline{C}_{33}$, $\overline{C}_{44}$, $\overline{C}_{55}$, and $\overline{C}_{66}$ of the prestressed body. After algebraic manipulation, the values given in any row of Table 1 lead us directly to that given in Table 2 in the row of the same number where the *Input data* are presented in the form suitable for inserting into Eqs. (23) – (28) in order to perform further calculations, with utilizing also Eq. (20). These calculations

are performed for the case when $r_1(\xi,\varphi,\phi)$, $r_3(\xi,\varphi,\phi)$, and $r_5(\xi,\varphi,\phi)$ are chosen as the three independent of each other functions $r_i(\xi,\varphi,\phi)$, i.e., when the analytical form of the function $p(\xi,\varphi,\phi)$ is given by Eq. (21). On inserting the values given in the respective row of Table 2 into Eqs. (23) – (28) and enclosing Eq. (20), we arrive at a system of nonlinear

Table 2.

Input data $[\mathrm{cm^2 s^{-2}}]$						
No	$H_{11}\cdot 10^{-11}$	$V_{33}^2\cdot 10^{-11}$	$V_{31}^2\cdot 10^{-11}$	$H_{22}\cdot 10^{-11}$	$V_{32}^2\cdot 10^{-11}$	$H_{12}\cdot 10^{-11}$
1	3.52304	3.45607	1.04044	3.50293	1.06056	0.993586
2	3.52303	3.45607	1.04043	3.50292	1.06054	0.993581
3	3.52301	3.45607	1.04042	3.50291	1.06052	0.993579
4	3.52286	3.45607	1.04035	3.50286	1.06035	0.993559
5	3.52267	3.45607	1.04026	3.50280	1.06013	0.993530
6	3.52248	3.45607	1.04016	3.50273	1.05991	0.993501
7	3.52230	3.45607	1.04007	3.50267	1.05970	0.993471
8	3.52117	3.45607	1.03951	3.50227	1.05841	0.993309
9	3.51930	3.45607	1.03857	3.50162	1.05625	0.993019

Table 3. Some results of numerical calculations.

No	L_1, L_3, L_5	$\overline{\sigma}_{11}\cdot 10^{-6}$ $[\mathrm{cm^2 s^{-2}}]$	$\overline{\sigma}_{22}/\overline{\sigma}_{11}$	Q_c	$q_{\min}\cdot 10^7$
1	$L_1 = -2.235763183772$ $L_3 = 1.0979886139440$ $L_5 = 0.5487668886877$	0.0	–	0.100859	3.184
2	$L_1 = -2.235960972127$ $L_3 = 1.0983295503730$ $L_5 = 0.5488253145014$	1.87084	0.4874	0.100992	4.879
3	$L_1 = -2.236795947828$ $L_3 = 1.0988891388090$ $L_5 = 0.5491093285845$	3.74168	0.4874	0.101234	4.879
4	$L_1 = -2.234641453048$ $L_3 = 1.1000725429550$ $L_5 = 0.5496786820460$	18.7084	0.4874	0.101991	4.892
5	$L_1 = -2.232686689108$ $L_3 = 1.1023022949130$ $L_5 = 0.5505769647418$	37.4169	0.4873	0.103102	2.746
6	$L_1 = -2.229401607267$ $L_3 = 1.1030163310740$ $L_5 = 0.5511099378546$	56.1252	0.4873	0.103932	4.894
7	$L_1 = -2.225893773403$ $L_3 = 1.1043245324470$ $L_5 = 0.5515539359085$	74.8337	0.4872	0.104756	4.871
8	$L_1 = -2.207377222687$ $L_3 = 1.111587495000$ $L_5 = 0.5551990370096$	187.84	0.4870	0.110156	4.875
9	$L_1 = -2.149780065096$ $L_3 = 1.104165497590$ $L_5 = 0.5570847777796$	374.168	0.4866	0.114811	4.880

equations of great complexity that are regarded by us as a reliable basis for evaluating numerically the partition function Z, the Lagrangian multipliers L_1, L_3, and L_5 together with the single-crystal effective material parameters $\overline{c}_{11}$, $\overline{c}_{12}$ and $\overline{c}_{44}$. Some of the results obtained by utilizing this algorithm are presented in Table 3, the others are presented in the forms of the diagrams in Figs. 1 – 10. All the numerical results are obtained for polycrystalline aggregate being under plane initial stress $\{\sigma^0_{11}, \sigma^0_{22}\}$ with the components $\sigma^0_{11} \geq 0$, $\sigma^0_{22} \simeq 0.487\sigma^0_{11}$ having successively the value of zero and eight different positive values.

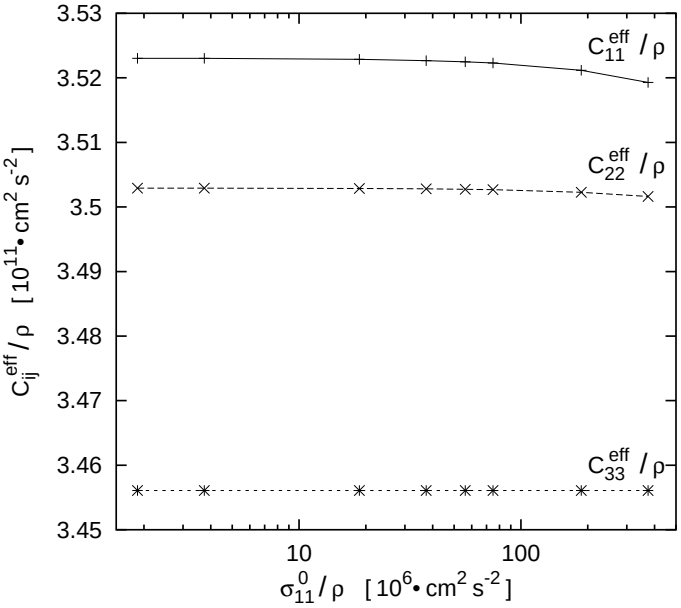

Fig. 1. C^{eff}_{11}/ρ, C^{eff}_{22}/ρ, and C^{eff}_{33}/ρ plotted against σ^0_{11}/ρ. On the horizontal (normalized initial stress σ^0_{11}/ρ) axis is set log scaling.

Solving the problem numerically, we have been encouraging in trying to do that by the implicit function theorem, which gives us only the hope, not certainty of satisfying seven nonlinear Eqs. (23) – (28), (20) in seven unknowns, Z, L_1, L_3, L_5, $\overline{c}_{11}$, $\overline{c}_{12}$ and $\overline{c}_{44}$, simultaneously. However, a set of nonlinear equations may have no (real) solutions at all or, contrariwise, it may have more than one solution, as it happens in each of the nine examples under consideration. In such nonlinear problems, solution finding invariably proceeds by iteration. Starting from some trial values of L_1, L_3, and L_5, a useful algorithm will improve the solution until some predetermined convergence criterions are satisfied, the solution being a set $\{Z, L_1, L_3, L_5, \overline{c}_{11}, \overline{c}_{12}, \overline{c}_{44}\}$. In order to have some check of the actual accuracy of calculation and the rate of convergence, a parameter Gm has been defined, the parameter Gm being a modification of that given in Ref. [9]:

$$Gm = \text{DMAX1}\,(G_{11}, G_{22}, G_{33}, G_{12}, G_{31}, G_{32}), \tag{29}$$

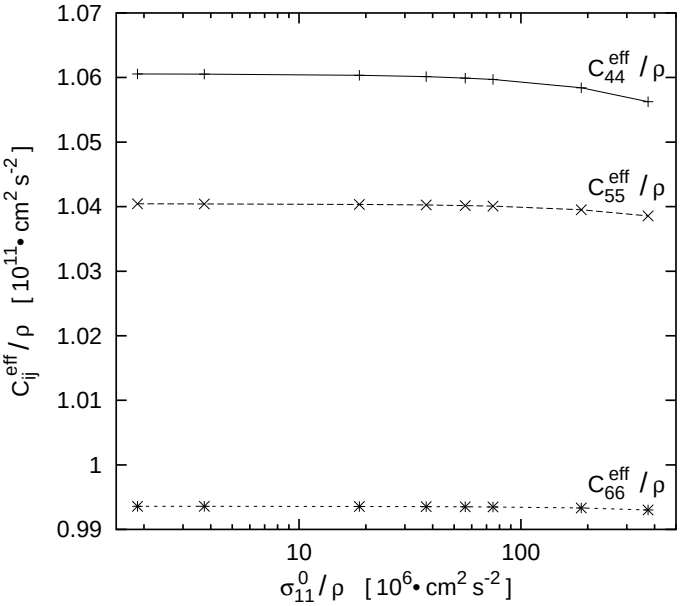

Fig. 2. C_{44}^{eff}/ρ, C_{55}^{eff}/ρ, and C_{66}^{eff}/ρ plotted against σ_{11}^0/ρ. On the horizontal (normalized initial stress σ_{11}^0/ρ) axis is set log scaling.

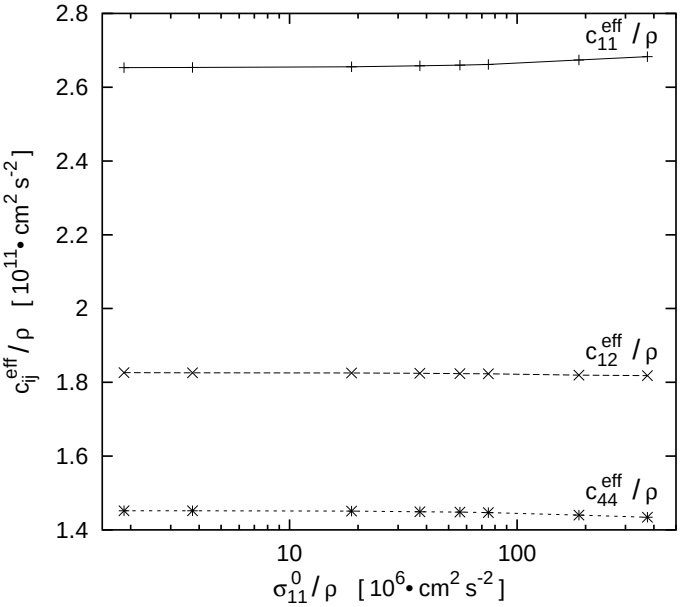

Fig. 3. c_{11}^{eff}/ρ, c_{12}^{eff}/ρ, and c_{44}^{eff}/ρ plotted against σ_{11}^0/ρ. On the horizontal (normalized initial stress σ_{11}^0/ρ) axis is set log scaling.

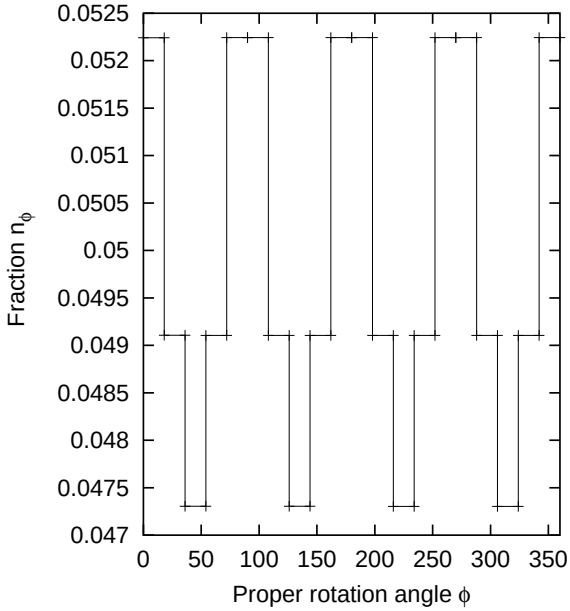

Fig. 4. Distribution of the particles $n_\phi(\phi_2, \phi_1)$ calculated from formula (34) for $\sigma^0_{11} = \sigma^0_{22} = 0$. The values of the angle of proper rotation (ϕ) are expressed in degrees.

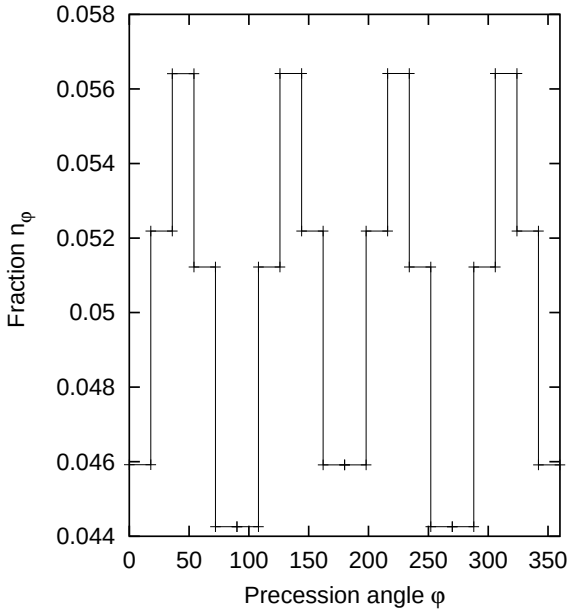

Fig. 5. Distribution of the particles $n_\varphi(\varphi_2, \varphi_1)$ calculated from formula (35) for $\sigma^0_{11} = \sigma^0_{22} = 0$. The values of the angle of precession (φ) are expressed in degrees.

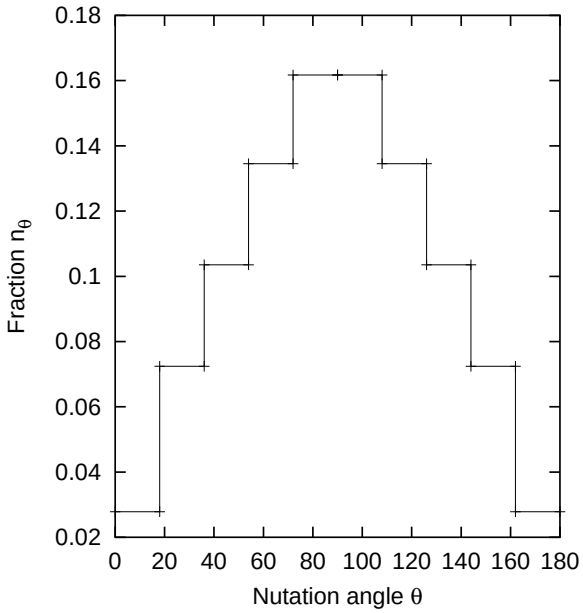

Fig. 6. Distribution of the particles $n_\theta(\theta_2, \theta_1)$ calculated from formula (36) for $\sigma^0_{11} = \sigma^0_{22} = 0$. The values of the angle of nutation (θ) are expressed in degrees.

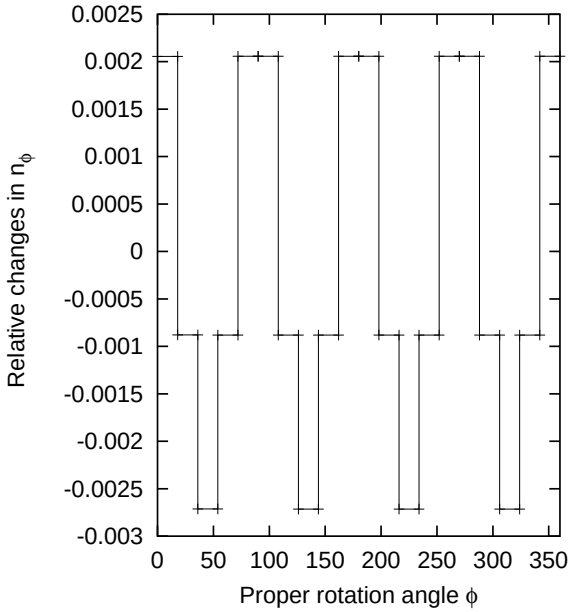

Fig. 7. The relative discrepancies between two histograms drawn for $n_\phi(\phi_2, \phi_1)$ at the limiting stresses: $\sigma^0_{11} = \sigma^0_{22} = 0$ and $\sigma^0_{11} = 3.74 \cdot 10^8\,\mathrm{cm^2 s^{-2}}$, $\sigma^0_{22} \simeq 0.487 \cdot \sigma^0_{11}$, the discrepancies being divided by the respective values of the histogram for $n_\phi(\phi_2, \phi_1)$ at $\sigma^0_{11} = \sigma^0_{22} = 0$. The values of the angle of nutation (ϕ) are expressed in degrees.

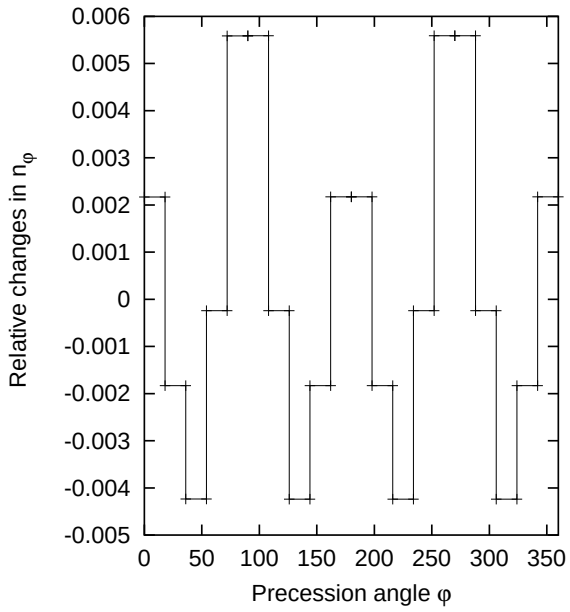

Fig. 8. The relative discrepancies between two histograms drawn for $n_{\varphi}(\varphi_2, \varphi_1)$ at the limiting stresses: $\sigma_{11}^0 = \sigma_{22}^0 = 0$ and $\sigma_{11}^0 = 3.74 \cdot 10^8\,\mathrm{cm^2 s^{-2}}$, $\sigma_{22}^0 \simeq 0.487 \cdot \sigma_{11}^0$, the discrepancies being divided by the respective values of the histogram for $n_{\varphi}(\varphi_2, \varphi_1)$ at $\sigma_{11}^0 = \sigma_{22}^0 = 0$. The values of the angle of nutation (φ) are expressed in degrees.

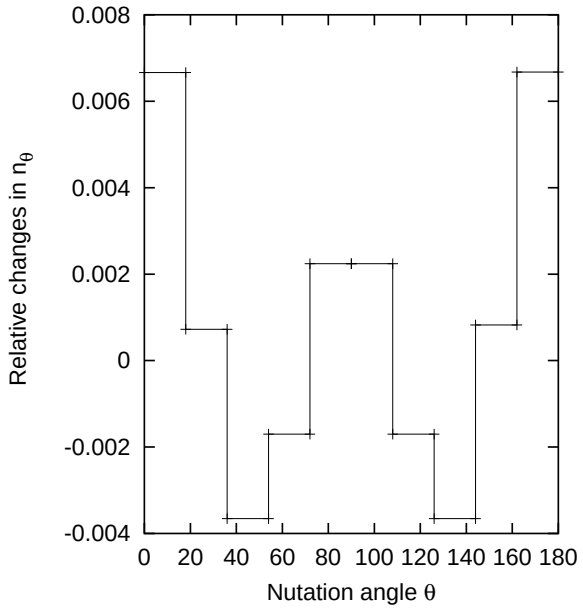

Fig. 9. The relative discrepancies between two histograms drawn for $n_{\theta}(\theta_2, \theta_1)$ at the limiting stresses: $\sigma_{11}^0 = \sigma_{22}^0 = 0$ and $\sigma_{11}^0 = 3.74 \cdot 10^8\,\mathrm{cm^2 s^{-2}}$, $\sigma_{22}^0 \simeq 0.487 \cdot \sigma_{11}^0$, the discrepancies being divided by the respective values of the histogram for $n_{\theta}(\theta_2, \theta_1)$ at $\sigma_{11}^0 = \sigma_{22}^0 = 0$. The values of the angle of nutation (θ) are expressed in degrees.

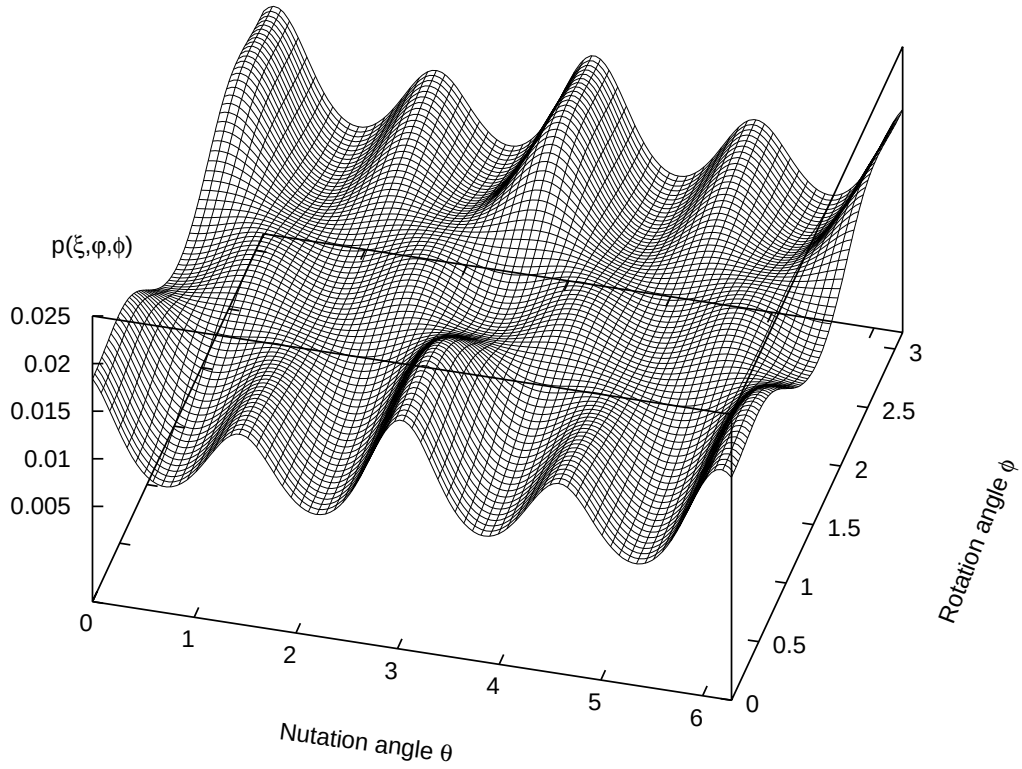

Fig. 10. Probability density function of the crystallite orientation, $p(\xi, \varphi, \phi)$, calculated together with c_{11}^{eff}, c_{12}^{eff}, and c_{44}^{eff} for the precession angle $\varphi = 0.3 \cdot \pi$ rad. The values of the angle of nutation (θ) and proper rotation (ϕ) are also expressed in radians.

where

$$
\begin{aligned}
G_{\alpha\beta} &= \text{DABS}\left[\left(H_{\alpha\beta}^{(\text{input})} - H_{\alpha\beta}^{(\text{deduced})}\right) / \text{DABS}\left(H_{\alpha\beta}^{(\text{input})}\right)\right], \quad \alpha\beta = 11, 12, 22, \\
G_{\gamma\delta} &= \text{DABS}\left[\left(H_{\gamma\delta}^{(\text{input})} - H_{\gamma\delta}^{(\text{deduced})}\right) / \text{DABS}\left(H_{\gamma\delta}^{(\text{input})}\right)\right], \\
H_{\gamma\delta}^{(\ldots)} &= \left(V_{\gamma\delta}^{(\ldots)}\right)^2, \qquad \gamma\delta = 31, 32, 33.
\end{aligned}
\tag{30}
$$

The superscripts (input) refers to the values of the quantities $H_{\alpha\beta}$, $H_{\gamma\delta}$ and $V_{\gamma\delta}^2$, which are given in the respective row of Table 2. As was mentioned, these values, which are the basis for determining (in the approximation of maximum Shannon entropy) the unknowns Z, L_1, L_3, L_5 (i.e., the function $p(\xi, \varphi, \phi)$) as well as $\overline{c}_{11}$, $\overline{c}_{12}$, $\overline{c}_{44}$, are regarded as experimental data (observables) obtained for the sample subjected to the initial plane stress σ_{ij}^0. Similarly, the superscripts (deduced) refer to the values of the quantities $H_{\alpha\beta}$ and $H_{\gamma\delta}$ which are deduced from Eqs. (23) – (28), (20), after inserting both the probability density function $p(\xi, \varphi, \phi)$ and the parameters $\overline{c}_{11}$, $\overline{c}_{12}$, $\overline{c}_{44}$ calculated from the observables in the former step. DMAX1 is the FORTRAN 77 intrisinc function, which

returns the maximum value in the argument list. The values of Gm for every set of input data, at which the respective iteration has been ended, are denoted by $q_{\min}$ and are listed in the sixth column of Table 3.

As was mentioned, each of the nine tasks of finding the unknowns Z, L_1, L_3, L_5, $\overline{c}_{11}$, $\overline{c}_{12}$ and $\overline{c}_{44}$ from Eqs. (23) – (28), (20) has more than one solution. This raises the need to provide a constructive criterion for making choice between numerous sets $\{Z, L_1, L_3, L_5, \overline{c}_{11}, \overline{c}_{12}, \overline{c}_{44}\}$ satisfying Eqs. (23) – (28), (20). Following Ref. [9], we make use herein of the criterion of the minimum value of the difference Q_c

$$Q_c = \mathrm{DMAX1}(Gc_{11}, Gc_{12}, Gc_{44}), \tag{31}$$

where

$$\begin{aligned} Gc_{ij} &= \mathrm{DABS}\left[\left(\overline{c}_{ij} - \overline{c}^0_{ij}\right)/\overline{c}^0_{ij}\right], \\ \overline{c}^0_{ij} &= c^0_{ij}/\rho^0, \qquad ij = 11, 12, 44. \end{aligned} \tag{32}$$

The values of the elastic stiffness moduli c^0_{11}, c^0_{12}, c^0_{44} and density ρ^0 of a single cubic crystal of the polycrystalline material (or a material as similar to that as possible) in the natural state (before deformation) are assumed to be known. Similarly as in Ref. [9], it is assumed that such a natural material for the rolled steel may be approximated by BCC Fe, which is characterized by the following values of $\overline{c}^0_{11}$, $\overline{c}^0_{12}$, and $\overline{c}^0_{44}$:

$$\begin{aligned} c^0_{11} &= 2.5982d + 07(m/s)^2, \\ c^0_{12} &= 1.6857d + 07(m/s)^2, \\ c^0_{44} &= 1.5843d + 07(m/s)^2. \end{aligned} \tag{33}$$

Now we formulate the criterion of minimum difference as the proposal of choosing this set of the values of Z, L_1, L_3, L_5, $\overline{c}_{11}$, $\overline{c}_{12}$, and $\overline{c}_{44}$ satisfying Eqs. (23) – (28), (20), which contains such values of the material parameters $\overline{c}_{11}$, $\overline{c}_{12}$, and $\overline{c}_{44}$ that lead to the minimum value of the difference parameter Q_c and simultaneously contains such values of Z, L_1, L_3, L_5 that lead to the probability density function $p(\xi, \varphi, \phi)$ achieving the maximum value of Shannon entropy. In each of the nine rows of the fifth column of Table 3, there is presented the value of the minimum difference Q_c corresponding to the solution $\{Z, L_1, L_3, L_5, \overline{c}_{11}, \overline{c}_{12}, \overline{c}_{44}\}$ of one of the nine examples under consideration. The first example concerns the situation where the material is not prestressed ($\sigma^0_{ij} = 0$). The full set $\{Z, L_1, L_3, L_5, \overline{c}_{11}, \overline{c}_{12}, \overline{c}_{44}\}$ for each of the nine examples (rows of Table 1) can be read in the following way: L_1, L_3, L_5 can be found in the respective row of the first column of Table 3, $\overline{c}_{11}$, $\overline{c}_{12}$, and $\overline{c}_{44}$ can be read out of Fig. 3 for each of the eight (No $= 2, 3, \ldots, 9$) prestressed states ($\sigma^0_{ij} \neq 0$) of the material. Since log scaling is set on the horizontal (normalized initial stress σ^0_{ij}/ρ) axis of each of Figs. 1 – 3, then the predicted values of material parameters $\overline{C}_{11}$, $\overline{C}_{22}$, $\overline{C}_{33}$, $\overline{C}_{44}$, $\overline{C}_{55}$, $\overline{C}_{66}$, $\overline{c}_{11}$, $\overline{c}_{12}$ and $\overline{c}_{44}$ of the non-prestressed body can not be indicated in Figs. 1 – 3. These values, expressed in $[10^{11}\,\mathrm{cm^2 s^{-2}}]$ units are as follows: 3.52304, 3.50293, 3.45607, 1.06056, 1.04044, 0.993586, 2.65267, 1.82618, 1.45220.

5. Discussion and conclusions

The data presented in the first column of Table 3 show the predicted changes in the values of the Lagrangian multipliers L_1, L_3 and L_5 with increasing stress components $\sigma_{11}^0 \geq 0$, $\sigma_{22}^0 \geq 0$ in the case when $\sigma_{22}^0/\sigma_{11}^0 \simeq 0.487$. For given L_1, L_3 and L_5, the partition function Z and, consequently, the function $p(\xi, \varphi, \phi)$ can also be regarded as a known quantity, since Z can be calculated immediately from the normalization condition (20). Therefore, the data presented in the first column of Table 3 enable us to estimate the influence of the increasing initial plane stress $\{\sigma_{11}^0, \sigma_{22}^0\}$ on the predicted texture of the polycrystalline aggregate under consideration. In order to visualize this effect, the quantities

$$n_\phi(\phi_2, \phi_1) \doteq \int_{\phi_1}^{\phi_2} \int_0^{2\pi} \int_{-1}^{1} p(\xi, \varphi, \phi)\, d\xi\, d\varphi\, d\phi, \tag{34}$$

$$n_\varphi(\varphi_2, \varphi_1) \doteq \int_0^{2\pi} \int_{\varphi_1}^{\varphi_2} \int_{-1}^{1} p(\xi, \varphi, \phi)\, d\xi\, d\varphi\, d\phi, \tag{35}$$

$$n_\theta(\theta_1, \theta_2) \doteq \int_0^{2\pi} \int_0^{2\pi} \int_{\xi_2}^{\xi_1} p(\xi, \varphi, \phi)\, d\xi\, d\varphi\, d\phi,$$

$$\theta_1 = \arccos \xi_1, \quad \theta_2 = \arccos \xi_2, \quad 0 \leq \theta_1 \leq \theta_2 \leq \pi \tag{36}$$

were calculated successively for L_1, L_3 and L_5 corresponding to the first and ninth sets $\{L_1, L_2, L_3\}$, which are written in the first and ninth rows of the first column of Table 3. The abbreviations, $n_\phi(\phi_2, \phi_1)$, $n_\varphi(\varphi_2, \varphi_1)$, and $n_\theta(\theta_2, \theta_1)$ denote the fractions of the total number of crystallites

(i) with the angle of proper rotation, ϕ, lying in the interval $\phi_1 \leq \phi \leq \phi_2$;

(ii) with the angle of precession, φ, lying in the interval $\varphi_1 \leq \phi \leq \varphi_2$, and

(iii) with the angle of nutation, θ, lying in the interval $\theta_1 \leq \theta \leq \theta_2$, respectively.

In Figs. 4 and 5, examples of numerical calculations of $n_\phi(\phi_2, \phi_1)$ and $n_\varphi(\varphi_2, \varphi_1)$, respectively, are presented for the case $\sigma_{11}^0 = \sigma_{22}^0$ with the whole domains $[0°, 360°]$ of the rotation angle ϕ and precession angle φ being divided into parts (subdomains) of equal size, 18°, with centres at $\phi = (\phi_1 - \phi_2)/2 = 9°, 27°, 45°, ..., 351°$ (Fig. 4) and at $\varphi = (\varphi_1 + \varphi_2)/2 = 9°, 27°, 45°, ..., 351°$ (Fig. 5). Similarly, in Fig. 6, an example of numerical calculations of $n_\theta(\theta_2, \theta_1)$ is presented for the same case $\sigma_{11}^0 = \sigma_{22}^0$ with the whole domain $[0°, 180°]$ of the nutation angle θ being divided into parts (subdomains) of equal size, 18°, with centres at $\theta = (\theta_1 + \theta_2)/2 = 9°, 27°, 45°, ..., 171°$. The crystallite fractions $n_\phi(\phi_2, \phi_1)$, $n_\varphi(\varphi_2, \varphi_1)$, and $n_\theta(\theta_2, \theta_1)$ were calculated separately for each subdomain and the results of these calculations are presented in the form of bar graphs (histograms) in Figs. 4–6. Results of numerical analysis show that the absolute values of the discrepancies between the elements of the histogram pairs, which correspond to the same subdomain of the same orientational angle ϕ, φ or θ but concern different initial stresses $\sigma_{11}^0 = \sigma_{22}^0 = 0$ or $\sigma_{11}^0 \neq 0$, $\sigma_{22}^0/\sigma_{11}^0 \simeq 0.487$, increases with increasing σ_{11}^0 (and σ_{22}^0). In this analysis,

$\overline{\sigma}^0_{11} = 3.74 \cdot 10^8\,\mathrm{cm^2 s^{-2}}$ and $\overline{\sigma}^0_{22} \simeq 0.487 \cdot \overline{\sigma}^0_{11}$ were the maximum values of the normalized plane stress $\{\overline{\sigma}^0_{11}, \overline{\sigma}^0_{22}\}$ under consideration. In Figs. 7–9, the values are presented of the relative discrepancies between elements of each of the three pairs of histograms $n_\phi(\phi_2, \phi_1)$, $n_\varphi(\varphi_2, \varphi_1)$, and $n_\theta(\theta_2, \theta_1)$, respectively, each of the histogram pairs being composed of two histograms for the same orientation angle ϕ, φ or θ and for the two limiting stresses: $\{\sigma^0_{11} = \sigma^0_{22} = 0\}$ and $\{\overline{\sigma}^0_{11} = 3.74 \cdot 10^8\,\mathrm{cm^2 s^{-2}}, \overline{\sigma}^0_{22} \simeq 0.487 \cdot \overline{\sigma}^0_{11}\}$. The relative discrepancy is defined for an angle subdomain as the ratio of the discrepancy in the subdomain between two histograms of the considered pair to the value of the histogram belonging to the same pair and concerning the case $\{\sigma^0_{11} = \sigma^0_{22} = 0\}$. The values of the relative discrepancies may be regarded as a measure of the effect of initial plane stress on the texture predicted by using the approach proposed in this paper. From Figs. 7–9 it can easily be seen that this effect for stress non greater than $\{\overline{\sigma}^0_{11} = 3.74 \cdot 10^8\,\mathrm{cm^2 s^{-2}}$, $\overline{\sigma}^0_{22} \simeq 0.487 \cdot \overline{\sigma}^0_{11}\}$ is revealed by the relative discrepancies smaller than 0.007 and therefore is negligibly small.

The increase of $\sigma^0_{ij} = \{\sigma^0_{11}, \sigma^0_{22}\} \neq 0$ also induces changes in the predicted normalized moduli $\overline{C}_{11}$, $\overline{C}_{22}$, $\overline{C}_{33}$, $\overline{C}_{44}$, $\overline{C}_{55}$, $\overline{C}_{66}$, $\overline{c}_{11}$, $\overline{c}_{12}$ and $\overline{c}_{44}$, which can be seen from Figs. 1–3. The maximum value of the relative changes in all the moduli (i.e., the changes in all the moduli divided by the values of the respective moduli of non-prestressed material) are smaller than 0.02, if $\overline{\sigma}^0_{11}$ increases from zero to about $374 \cdot 10^6\,\mathrm{cm^2 s^{-2}}$. For the steel of the density $\rho = 7.819\,\mathrm{g\,cm^{-3}}$, it denotes the changes in the value of σ^0_{11} lying in the interval from zero to about 292 MPa. This value is a typical one of residual stress in steel being plastically deformed (e.g., rolled). Hence we can conclude that for rolled steel the changes in the predicted values of the considered moduli, which are induced by the considered residual stress, are negligibly small.

References

[1] Tatsuo Tokuoka and Yukio Iwashimizu, *Acoustical birefringence of ultrasonic waves in deformed isotropic elastic materials*, Int. J. Solids Structures, **4**, 383–389 (1968).

[2] C.S. Man and W.Y. Lu, *Towards an acoustoelastic theory for measurement of residual stress*, Journal of Elasticity, **17**, 159–182 (1987).

[3] C.M. Sayers, *Ultrasonic velocities in anisotropic polycrystalline aggregates*, J. Phys.D: Appl. Phys., **15**, 2157–2167 (1982).

[4] R.B. Thomson, S.S. Lee and J.F. Smith, *Angular dependence of ultrasonic wave propagation in a stressed, orthorhombic continuum: Theory and application to the measurement of stress and texture*, J. Acoust. Soc. Am., **80**, 3, 921–931 (1986).

[5] A.D. Degtyar and S.I. Rokhlin, *Absolute stress determination in orthotropic materials from angular dependences of ultrasonic velocities*, J. Appl. Phys., **78**, 3, 1547–1556 (1995).

[6] W. Voigt, *Lehrbuch der Krystall Physik*, Teubner, Leipzig 1928.

[7] E.T. Jaynes, *Information theory and statistical mechanics*, Phys. Rev., **106**, 620–630 (1957).

[8] J. Lewandowski, *Maximum-entropy estimate of the orthorhombic texture from ultrasonic measurements*, Ultrasonics, 229–238 (1995).

[9] J. Lewandowski, *Determination of material parameters and texture of a polycrystalline aggregate from ultrasonic measurements*, NDT&E International, **32**, 383–396 (1999).

[10] E. Kroner, *Statistical continuum mechanics*, Lecture Notes, Springer, Berlin 1971.

[11] I. Ignberg, *Residual macrostresses in thin strip production*, [in:] Swedish Symposium on Residual Stresses, T. Ericsson, J. Bergstrom, I. Nyman [Eds.], March 30-April 2, 1987, 33–55.

[12] A. Reuss, Z. Angew: Math. Mech., **9**, 49, (1924).

[13] R.J. Hill, Mech. Phys. Solids, 5, 229 (1957).